JINR-E2-2005-21, RUB-TPII-10/04

Renormalization-group improved evolution of the meson distribution amplitude at the two-loop level

Alexander P. Bakulev*

Bogoliubov Laboratory of Theoretical Physics,
Joint Institute for Nuclear Research,
141980, Moscow Region, Dubna, Russia

N. G. Stefanis†

Institut für Theoretische Physik II
Ruhr-Universität Bochum
D-44780 Bochum, Germany

(Dated: February 2, 2008)

Abstract

We discuss the two-loop evolution of the flavor-nonsinglet meson distribution amplitude in perturbative QCD. After reviewing previous two-loop computations, we outline the incompatibility of these solutions with the group property of the renormalization-group transformations. To cure this deficiency, we compute a correction factor for the non-diagonal part of the meson evolution equation and prove that with this modification the two-loop solution conforms with the group properties of the renormalization-group transformations. The special case of a fixed strong coupling (no Q^2 dependence) is also discussed and comparison is given to previously obtained results.

PACS numbers: 11.10.Hi,12.38.Bx,11.25.Hf,12.38.Lg

Keywords: evolution equation, pion distribution amplitude, renormalization group equation, conformal symmetry

*Electronic address: bakulev@thsun1.jinr.ru

†Electronic address: stefanis@tp2.ruhr-uni-bochum.de

I. INTRODUCTION

In order to use perturbative QCD (pQCD) for the description of exclusive processes, one usually appeals to factorization theorems, which ensure that the pQCD calculable information, described by the so-called hard scattering amplitude, $T_{\rm H}$, can be factored out at a factorization scale $\mu_{\rm F}^2$, whereas all pQCD non-calculable (i.e., non-perturbative) contributions are encoded in terms of universal hadron distribution amplitudes (DA)s, φ_h. Schematically, this can be illustrated for the case of the $\gamma^*\gamma^* \to \pi$ transition form factor in the following way:

$$F_{\gamma^*\gamma^*\to\pi}(Q^2,q^2) = f_\pi T_{\rm H}(x;Q^2,q^2,\mu_{\rm F}^2) \underset{x}{\otimes} \varphi_\pi(x;\mu_{\rm F}^2)\,, \tag{1.1}$$

where Q^2 and q^2 are the photon virtualities and $\otimes$ denotes the usual convolution symbol ($A(x) \underset{x}{\otimes} B(x) \equiv \int_0^1 dx A(x)B(x)$) over the longitudinal momentum fraction variable x. The dependence of the DA $\varphi_\pi(x;\mu_{\rm F}^2)$ on the factorization scale $\mu_{\rm F}^2$ is governed by the Efremov–Radyushkin–Brodsky–Lepage (ERBL) evolution equation [1, 2]

$$\frac{d\,\varphi_\pi(x;\mu_{\rm F}^2)}{d\,\ln\mu_{\rm F}^2} \;=\; V(x,u;\alpha_s(\mu_{\rm F}^2)) \underset{u}{\otimes} \varphi_\pi(u;\mu_{\rm F}^2) \tag{1.2}$$

with the evolution kernel

$$V(x,u;\alpha_s(\mu^2))) \;=\; \left(\frac{\alpha_s(\mu^2))}{4\pi}\right) V_0(x,y) + \left(\frac{\alpha_s(\mu^2))}{4\pi}\right)^2 V_2(x,y) + \dots\,, \tag{1.3}$$

adopting the notation of [3]. The one-loop evolution kernel V_0 was introduced in Ref. [2]; an analogous expression for V_2 at the two-loop level was derived in Refs. [4, 5, 6, 7]. If factorization applies, it is, in principle, safe and legitimate to use different values of $\mu_{\rm F}^2$, dispensing with the factorization-scale dependence by means of the renormalization group. Usually, one sets $\mu_{\rm F}^2 = \bar{Q}^2 \equiv Q^2 + q^2$ in order to eliminate in $T_{\rm H}$ large logarithms of the type $\ln(\bar{Q}^2/\mu_{\rm F}^2)$ and for that reason one then needs to evolve the meson DA $\varphi_\pi(x;\mu^2)$ in accordance with Eq. (1.2) from a low normalization point $\mu_0^2 \lesssim 1$ GeV^2, at which the pion DA has been (non-perturbatively) determined, to a higher scale $\mu^2 = \bar{Q}^2$ at which comparison with experimental data may be attempted.

The structure of the two-loop evolution kernel was analyzed by Mikhailov and Radyushkin (MR) in [3] and its diagonality violating terms (in the Gegenbauer basis) were identified, though their origin remained partly unclear. Moreover, the two-loop evolution with Q^2 of any pion DA at the reference (or initial) momentum μ_0^2 was carried out numerically, but including only the first few expansion coefficients at order α_s^2. On that basis, these authors concluded that the next-to-leading-order (NLO) correction to the pion DA with $\mu_0^2 \simeq 1$ GeV^2 and at $x = 0.5$ remains less than a few percent even for momenta far beyond 10^2 GeV^2. Later, the two-loop evolution of the pion DA was studied by Müller in [8] using conformal constraints. In this work, a complete formal solution in NLO was obtained with the inclusion of all two-loop mixing coefficients. This solution was further discussed in [9] for a running and also a fixed coupling constant. It was found that the NLO correction can be rather large – especially for endpoint-concentrated DAs, like the Chernyak–Zhitnitsky (CZ) [10] one, supplying logarithmic enhancement exactly in this region.

However, as we will show below, all these solutions violate the group character of the renormalization-group (RG) evolution transformations to the order α_s^2. Whether it is possible

to obtain an approximate solution of the evolution equation that, nevertheless, respects its group properties, remains an open question. It is exactly this issue to which the present work is devoted. Such an improvement is not only theoretically important, it is also of practical concern since the modification of the evolution behavior, entailed by the restoration of the RG properties, will have influence on measurable hadronic observables, like meson form factors.

In the next section, we shall briefly review the main properties of the two-loop approximation of the QCD coupling and describe the standard formalism for the DA evolution at the two-loop level. Section III presents the analysis of the RG transformation when the second and higher Gegenbauer harmonics are taken into account. A semi-explicit solution of the two-loop evolution equation that preserves the RG structure is constructed in Sec. IV. In Sec. V we discuss the numerical importance of the obtained solution. The special case of a fixed coupling constant is treated in Sec. VI, while some important technical details are collected in two appendixes.

II. QCD COUPLING AND EVOLUTION OF THE PION DA AT NLO

A. Standard formalism with standard notations

To illustrate the "RG philosophy" and clarify the objective of this work, let us recall the Ovsyannikov–Callan–Symanzik equation for the (running) coupling, $\alpha_s\,(Q^2)$, in QCD:

$$\frac{d\alpha_s\,(Q^2)}{d\ln(Q^2)} = \beta\left(\alpha_s(Q^2)\right)\,. \tag{2.1}$$

Strictly speaking, $\alpha_s(Q^2)$ and also $\beta(\alpha_s(Q^2))$ depend on the number of active flavors, N_f. For the considerations to follow, this will not be important and hence we omit the N_f-dependence any further. The β-function in the NLO approximation is given by

$$\beta\,(\alpha_s) = -\frac{\alpha_s^2}{4\pi}\left(b_0 + b_1\frac{\alpha_s}{4\pi}\right)\,, \tag{2.2}$$

where the standard β-function coefficients are provided in Appendix A. The two-loop equation for $\alpha_s(Q^2)$ (with $\Lambda_{\rm QCD}\equiv\Lambda$) reads

$$\frac{4\pi}{b_0\alpha_s(Q^2)} - c_1\ln\left[\frac{4\pi}{b_0\alpha_s(Q^2)} + c_1\right] = \ln\left(\frac{Q^2}{\Lambda^2}\right) \quad \text{with } c_1\equiv b_1/b_0^2\,. \tag{2.3}$$

The solution of this equation can be written in terms of the Lambert W_{-1}-function with the argument $\zeta(Q^2)\equiv-\frac{1}{ec_1}\left(\frac{\Lambda^2}{Q^2}\right)^{1/c_1}$ to obtain

$$\alpha_s^{\text{2-loop}}\left(Q^2\right) \;=\; -\frac{4\pi}{b_0\,(N_f)\,c_1\,[1+W_{-1}(\zeta(Q^2))]}\,, \tag{2.4}$$

as it was shown in [11, 12].

Now let us turn to the ERBL evolution equation for the meson DA. First, we recall the main properties of the one-loop approximation. (See Ref. [13] for a pedagogical exposition and further references.) The one-loop evolution kernel has a very simple structure, viz.,

$$V_{\text{1-loop}}(x,y;\alpha_s) \;=\; \frac{\alpha_s}{4\pi}V_0(x,y) \tag{2.5}$$

with factorizing α_s- and x-dependences. The formal solution of the ERBL equation in the one-loop approximation is

$$\varphi_\pi(x;\mu_0^2) \stackrel{\text{ERBL}}{\longrightarrow} \varphi_\pi^{\text{1-loop}}(x;Q^2) \;=\; \exp\left[\int_{\alpha_s(\mu_0^2)}^{\alpha_s(Q^2)} \frac{\alpha_s V_0}{4\pi\beta_1(\alpha)} d\alpha \otimes\right] \varphi_\pi(x;\mu_0^2)\,, \tag{2.6}$$

where $\beta_1(\alpha) = -b_0\alpha_s^2/(4\pi)$ is the one-loop β-function and the exponent above has to be evaluated according to $\Big[V_0 \otimes\Big]^n \varphi_\pi(x;\mu_0^2) = V_0(x,u_1) \underset{u_1}{\otimes} \ldots \underset{u_{n-1}}{\otimes} V_0(u_{n-1},u_n) \underset{u_n}{\otimes} \varphi_\pi(u_n;\mu_0^2)$. It is useful to expand the meson DA[1]

$$\varphi_\pi(x;Q^2) \;=\; \Omega(x) {\sum_{n\geq 0}}' a_n(Q^2)\cdot\psi_n(x) \tag{2.7}$$

in terms of the eigenfunctions $\Omega(x)\psi_n(x)$ of the one-loop ERBL kernel (2.5), i.e., in terms of the Gegenbauer polynomials $C_n^{3/2}(\xi)$,

$$\Omega(x) \;\equiv\; 6\,x(1-x)\,, \qquad \psi_n(x) \;\equiv\; C_n^{3/2}(2x-1)\,, \tag{2.8}$$

corresponding to the eigenvalues

$$\gamma_n^{\text{1-loop}}(\alpha_s) = \frac{-1}{2}\left(\frac{\alpha_s}{4\pi}\right)\gamma_0(n) \tag{2.9}$$

with $\gamma_0(n)$ given in Appendix A. In this representation all the dependence on Q^2 is contained in the coefficients $a_n(Q^2)$:

$$a_n^{\text{1-loop}}(Q^2) \;=\; a_n(\mu_0^2)\left[\frac{\alpha_s(Q^2)}{\alpha_s(\mu_0^2)}\right]^{\gamma(n)} \quad \text{with} \quad \gamma(n) \;\equiv\; \frac{\gamma_0(n)}{2b_0}\,. \tag{2.10}$$

This simple scheme is due to the special factorized structure of the one-loop evolution kernel (2.5). In the two-loop approximation this is no more the case. Indeed, the evolution kernel

$$V_{\text{2-loop}}(x,y;\alpha_s(\mu^2)) \;=\; \left(\frac{\alpha_s(\mu^2)}{4\pi}\right) V_0(x,y) + \left(\frac{\alpha_s(\mu^2)}{4\pi}\right)^2 V_2(x,y) \tag{2.11}$$

has, at each scale μ^2, different eigenfunctions, which explicitly depend on $\alpha_s(\mu^2)$. Nevertheless, these eigenfunctions of the two-loop ERBL kernel can also be expanded in terms of the one-loop eigenfunctions $\Omega(x)\psi_n(x)$. In this basis, the two-loop kernel (2.11) can be represented in a matrix form of a triangular type:

$$V_{\text{2-loop}}(x,y;\alpha_s) \;=\; \Omega(x) {\sum_n}' {\sum_j}' \psi_n(x) \frac{V_{\text{2-loop}}^{n,j}(\alpha_s)}{N_j} \psi_j(y)\,; \tag{2.12}$$

$$V_{\text{2-loop}}^{n,j}(\alpha_s) \;=\; \frac{-1}{2}\left(\frac{\alpha_s}{4\pi}\right)\left\{\gamma_0(n)\delta_{n,j} + \left(\frac{\alpha_s}{4\pi}\right)\left[\gamma_1(n)\delta_{n,j} - M_{j,n}\theta(j<n)\right]\right\} \tag{2.13}$$

[1] Here ${\sum_{n>0}}'$ denotes the sum over even indices $n>0$ only in order to account for the symmetry relation $\varphi_\pi(x;Q^2) = \varphi_\pi(1-x)$ due to charge-conjugation invariance and isospin symmetry.

with normalization coefficients N_j, next-to-leading order anomalous dimensions $\gamma_1(n)$, and off-diagonal matrix elements $M_{j,n}$ given in Appendix A .

We see that the diagonal terms in Eq. (2.13), $V^{n,n}_{\text{2-loop}}(\alpha_s)$, define the anomalous dimensions

$$\gamma_n(\alpha_s) \;=\; \frac{-1}{2}\left(\frac{\alpha_s}{4\pi}\right)\left[\gamma_0(n) + \left(\frac{\alpha_s}{4\pi}\right)\gamma_1(n)\right], \tag{2.14}$$

whereas the off-diagonal terms, $V^{n,j\neq n}_{\text{2-loop}}(\alpha_s) \sim \alpha_s^2 M_{j,n}$, define the mixing of higher harmonics. Solutions of the evolution equation at the two-loop level have been given in [3, 8, 14], and have the form

$$\varphi_\pi^{\text{2-loop}}(x,Q^2) = \Omega(x)\sum_n{}' a_n(\mu_0^2)E_n(Q^2,\mu_0^2)\left[\psi_n(x) + \frac{\alpha_s(Q^2)}{4\pi}\sum_{j>n}{}' d_{n,j}(Q^2,\mu_0^2)\psi_j(x)\right] \tag{2.15}$$

so that the evolved coefficients are

$$a_n^{\text{2-loop}}(Q^2) \;=\; E_n(Q^2,\mu_0^2)a_n(\mu_0^2) + \frac{\alpha_s(Q^2)}{4\pi}\sum_{0\le j<n}{}' E_j(Q^2,\mu_0^2)d_{j,n}(Q^2,\mu_0^2)a_j(\mu_0^2)\,. \tag{2.16}$$

Here, the "diagonal" part $E_n(Q^2,\mu_0^2)$ is the *exact* part of this solution, namely,

$$E_n(Q^2,\mu_0^2) \;=\; \frac{e_n(Q^2)}{e_n(\mu_0^2)}; \qquad e_n(Q^2) \;=\; \Big[\alpha_s(Q^2)\Big]^{\gamma(n)}\Big[1+\delta_1\alpha_s(Q^2)\Big]^{\omega(n)}, \tag{2.17}$$

$$\delta_1 \;\equiv\; \frac{b_1}{4\pi b_0}; \qquad \omega(n) \;\equiv\; \frac{\gamma_1(n)b_0 - \gamma_0(n)b_1}{2b_0b_1}, \tag{2.18}$$

while the "non-diagonal" part is considered in the NLO approximation. Note that the coefficients $d_{n,j}(Q^2,\mu_0^2)$ are related to the off-diagonal matrix elements (2.13) and fix the mixing of the higher, $j>n$, harmonics in (2.15).

In the MR solution these coefficients are given by

$$d_{j,n}^{\text{MR}}(Q^2,\mu_0^2) \;=\; \frac{M_{j,n}}{2b_0\big[\gamma(n)-\gamma(j)-1\big]}\left\{1 - \left[\frac{\alpha_s(Q^2)}{\alpha_s(\mu_0^2)}\right]^{\gamma(n)-\gamma(j)-1}\right\}. \tag{2.19}$$

As we shall see in the next sections, the approximate MR coefficients $d_{j,n}^{\text{MR}}(Q^2,\mu_0^2)$ explicitly violate the group property of the RG transformation at the $O(\alpha_s)$-level.

B. Standard formalism with modified notations

It turns out to be more convenient to rewrite the main equations of the previous subsection in terms of the modified notations, $\gamma(n)$ (Eq. (2.10)), δ_1, and $\omega(n)$ (Eq. (2.18)). Then, the β-function becomes

$$\beta\left(\alpha_s\right) = -b_0\frac{\alpha_s^2}{4\pi}\left[1+\delta_1\alpha_s\right]. \tag{2.20}$$

Next, the two-loop kernel reads

$$V^{n,j}_{\text{2-loop}}(\alpha_s) = -b_0\left(\frac{\alpha_s}{4\pi}\right)\left\{\left[\gamma(n)\left(1+\delta_1\alpha_s\right) + \omega(n)\delta_1\alpha_s\right]\delta_{n,j} - \frac{\alpha_s}{8\pi b_0}M_{j,n}\theta(j<n)\right\}. \tag{2.21}$$

Finally, we rewrite the two-loop ERBL equations (1.2), (2.12), (2.13) using the representation (2.7) and changing variables from Q^2 to α_s with the help of Eqs. (2.1) to derive

$$\beta(\alpha_s)\frac{da_n(\alpha_s)}{d\alpha_s} = \frac{-1}{2}\left(\frac{\alpha_s}{4\pi}\right)\left[\left(\gamma_0(n) + \frac{\alpha_s}{4\pi}\gamma_1(n)\right)a_n(\alpha_s) - \frac{\alpha_s}{4\pi}{\sum_{0\le j<n}}' M_{j,n}a_j(\alpha_s)\right]. \quad (2.22)$$

After taking into account Eqs. (2.20) and (2.21), this expression gives

$$\alpha_s\left(1+\delta_1\alpha_s\right)\frac{da_n(\alpha_s)}{d\alpha_s} = \left[\gamma(n)\left(1+\delta_1\alpha_s\right) + \omega(n)\delta_1\alpha_s\right]a_n(\alpha_s) - \alpha_s{\sum_{0\le j<n}}'\tilde{m}_{n,j}a_j(\alpha_s)\,, \quad (2.23)$$

where we have defined the reduced matrix elements $\tilde{m}_{n,j} \equiv M_{j,n}/(8\pi b_0)$. These expressions are going to be helpful in deriving an exact RG solution in Sec. IV.

III. GROUP PROPERTY OF THE RENORMALIZATION GROUP TRANSFORMATION FOR GEGENBAUER HARMONICS

In this section we consider exclusively the two-loop evolution equation given by expressions (1.2) and (2.11). For this reason, we omit in the following all two-loop-superscripts. We want to understand if the approximate form (2.15) respects the group property of the RG transformation, that is,

$$U(Q^2,q^2)\cdot U(q^2,\mu^2) = U(Q^2,\mu^2)\,; \quad (3.1)$$

if not, we want to estimate to what extent it violates it.

A. The second harmonic

To this end, let us consider first the evolution of the Gegenbauer coefficient a_2. According to (2.16), we have

$$a_2(\mu_0^2) \to a_2(Q^2) \;\equiv\; U(Q^2,\mu_0^2)a_2(\mu_0^2) \;=\; E_2(Q^2,\mu_0^2)\,a_2(\mu_0^2) + D_{20}(Q^2,\mu_0^2)\,, \quad (3.2)$$

where we defined $D_{20}(Q^2,\mu^2) \equiv (\alpha_s(Q^2)/4\pi)d_{02}(Q^2,\mu^2)$. If group property (3.1) is valid, then it follows

$$E_2(Q^2,q^2)\big[E_2(q^2,\mu^2)a_2(\mu^2) + D_{20}(q^2,\mu^2)\big] + D_{20}(Q^2,q^2) = E_2(Q^2,\mu^2)a_2(\mu^2) + D_{20}(Q^2,\mu^2)$$

and from the arbitrariness of $a_2(\mu^2)$ one gets

$$E_2(Q^2,\mu^2) \;=\; E_2(Q^2,q^2)E_2(q^2,\mu^2)\,; \quad (3.3)$$

$$D_{20}(Q^2,\mu^2) \;=\; E_2(Q^2,q^2)D_{20}(q^2,\mu^2) + D_{20}(Q^2,q^2)\,. \quad (3.4)$$

The first equation is satisfied identically by virtue of Eq. (2.17). The second one is more complicated, but can be readily proved. Define a function $Z_{20}(Q^2,\mu^2)$ by

$$D_{20}(Q^2,\mu^2) \;=\; e_2(Q^2)Z_{20}(Q^2,\mu^2)\,. \quad (3.5)$$

Then, Eq. (3.4) implies

$$Z_{20}(Q^2,\mu^2) \;=\; Z_{20}(Q^2,q^2) + Z_{20}(q^2,\mu^2)\,. \quad (3.6)$$

The general solution of this functional equation is just

$$Z_{20}(Q^2,\mu^2) \;=\; \Psi_{20}(Q^2) - \Psi_{20}(\mu^2) \tag{3.7}$$

for some auxiliary function $\Psi_{20}(\mu^2)$. In order to find the explicit form of $\Psi_{20}(\mu^2)$, one has to use evolution equation (2.23), what we will conduct in Sec. IV. By using the MR approximate solution (2.19), we see that it generates the function

$$D_{20}^{\rm MR}(Q^2,\mu^2) \;=\; \left[\alpha_s(Q^2)\right]^{\gamma(2)} \left[\Psi_{20}(Q^2) - \Psi_{20}(\mu^2)\right] \tag{3.8}$$

with

$$\Psi_{20}(\mu^2) \;=\; \frac{\tilde{m}_{20}}{(\gamma(2)-1)\,[\alpha_s(\mu^2)]^{\gamma(2)-1}}\,. \tag{3.9}$$

From this, we conclude that in order that $D_{20}^{\rm RG}(Q^2,\mu^2)$ is consistent with the RG transformation property, it has to be given by

$$D_{20}^{\rm RG}(Q^2,\mu^2) \;=\; e_2(Q^2)\Big[\Psi_{20}(Q^2) - \Psi_{20}(\mu^2)\Big]\,. \tag{3.10}$$

Comparing (3.8) with (3.10) leads us to the conclusion that the group property of the RG transformations in the MR approximate form is violated because the factor $\left[1+\delta_1\alpha_s(Q^2)\right]^{\omega(2)}$ is missing. Evidently, this violation is of $O(\alpha_s)$.

B. The nth harmonic

The next task is to generalize these results to the case of arbitrary polynomial order $n = 2, 4, \ldots$. To achieve this, we define $D_{nk}(Q^2,\mu^2)$ and $Z_{nk}(Q^2,\mu^2)$ as

$$D_{n,j}(Q^2,\mu^2) \;\equiv\; \frac{\alpha_s(Q^2)}{4\pi} E_j(Q^2,\mu^2) d_{j,n}(Q^2,\mu^2) \;=\; e_n(Q^2) Z_{n,j}(Q^2,\mu^2) e_j(\mu^2)^{-1}\,; \tag{3.11}$$

$$Z_{n,j}(Q^2,\mu^2) \;=\; \frac{\alpha_s(Q^2)}{4\pi} e_j(Q^2) d_{j,n}(Q^2,\mu^2) e_n(Q^2)^{-1}\,. \tag{3.12}$$

Then, the evolution of the Gegenbauer coefficient a_n from the scale μ^2 to the scale Q^2 in accordance with Eq. (2.16) is given by

$$a_n(Q^2) \;=\; e_n(Q^2)\left[a_n(\mu^2)e_n^{-1}(\mu^2) + {\sum_{0\le j<n}}' Z_{n,j}(Q^2,\mu^2)\, a_j(\mu^2) e_j^{-1}(\mu^2)\right]. \tag{3.13}$$

The group property (3.1) dictates

$$\begin{aligned}{\sum_{0\le j<n}}' Z_{n,j}(Q^2,\mu^2)\, a_j(\mu^2) e_j(\mu^2)^{-1} = {\sum_{0\le j<n}}' \left[Z_{n,j}(Q^2,q^2) + Z_{n,j}(q^2,\mu^2)\right]\, a_j(\mu^2) e_j^{-1}(\mu^2) \\ + {\sum_{0\le j<n}}' {\sum_{0\le k<j}}' Z_{n,j}(Q^2,q^2) Z_{jk}(q^2,\mu^2)\, a_k(\mu^2) e_k^{-1}(\mu^2)\end{aligned} \tag{3.14}$$

and from the arbitrariness of $a_j(\mu^2)$ we obtain

$$Z_{n,j}(Q^2,\mu^2) \;=\; Z_{n,j}(Q^2,q^2) + Z_{n,j}(q^2,\mu^2) + {\sum_{n>k>j}}' Z_{nk}(Q^2,q^2) Z_{kj}(q^2,\mu^2)\,. \tag{3.15}$$

1. The case $j = n - 2$

For $j = n - 2$ we have the complete analogue of Eq. (3.6), i.e.,

$$Z_{n,n-2}(Q^2,\mu^2) \;=\; Z_{n,n-2}(Q^2,q^2) + Z_{n,n-2}(q^2,\mu^2) \tag{3.16}$$

yielding the exact solution

$$Z_{n,n-2}(Q^2,\mu^2) \;=\; \Psi_{n,n-2}(Q^2) - \Psi_{n,n-2}(\mu^2)\,. \tag{3.17}$$

2. The case $j = n - k$ with arbitrary and even $k < n$

Let us rewrite Eq. (3.15) in the more appropriate form

$$\begin{aligned} Z_{n,n-k}(Q^2,\mu^2) \;&=\; Z_{n,n-k}(Q^2,q^2) + Z_{n,n-k}(q^2,\mu^2) \\ &+ \sum_{0<j<k}{}' Z_{n,n-j}(Q^2,q^2) Z_{n-j,n-k}(q^2,\mu^2)\,. \end{aligned} \tag{3.18}$$

Using the principle of mathematical induction, we can prove that

$$Z_{n,n-k}(Q^2,\mu^2) = \Psi_{n,n-k}(Q^2) - \Psi_{n,n-k}(\mu^2) - \sum_{0<j<k}{}' Z_{n,n-j}(Q^2,\mu^2)\Psi_{n-j,n-k}(\mu^2) \tag{3.19}$$

is the solution of Eq. (3.18) (relegating further details to Appendix B).

We are now in the position to summarize our findings and rewrite the solution of the NLO evolution equation (1.2) in the form (2.7) with the nth Gegenbauer coefficient that respects the RG properties being given by

$$a_n^{\rm RG}(\mu^2) \;=\; e_n(\mu^2)\left[a_n(\mu_0^2)e_n^{-1}(\mu_0^2) + \sum_{0\le j<n}{}' Z_{n,j}^{\rm RG}(\mu^2,\mu_0^2)\, a_j(\mu_0^2)e_j^{-1}(\mu_0^2)\right], \tag{3.20}$$

where

$$e_n(\mu^2) \;=\; \Big[\alpha_s(\mu^2)\Big]^{\gamma(n)}\Big[1+\delta_1\alpha_s(\mu^2)\Big]^{\omega(n)}; \tag{3.21}$$

$$Z_{n,k}^{\rm RG}(\mu^2,\mu_0^2) \;=\; \Psi_{n,k}(\mu^2) - \Psi_{n,k}(\mu_0^2) - \sum_{n>j>k}{}' Z_{n,j}^{\rm RG}(\mu^2,\mu_0^2)\Psi_{j,k}(\mu_0^2)\,, \tag{3.22}$$

with $\Psi_{n,j}(\mu^2)$ being defined on account of evolution equation (2.23), a task we will conduct in Sec. IV.

It is instructive to rewrite the approximate MR solution in an analogous manner to obtain

$$a_n^{\rm MR}(\mu^2) \;=\; e_n(\mu^2)\left[a_n(\mu_0^2)e_n^{-1}(\mu_0^2) + \sum_{0\le j<n}{}' Z_{n,j}^{\rm MR}(\mu^2,\mu_0^2) a_j(\mu_0^2)e_j^{-1}(\mu_0^2)\right]; \tag{3.23}$$

$$\begin{aligned} Z_{n,k}^{\rm MR}(\mu^2,\mu_0^2) \;&\equiv\; \frac{e_k(\mu^2)\alpha_s(\mu^2)^{\gamma(n)}}{e_n(\mu^2)\alpha_s(\mu^2)^{\gamma(k)}}\left[\Psi_{n,k}^{\rm MR}(\mu^2) - \Psi_{n,k}^{\rm MR}(\mu_0^2)\right] \\ &=\; \left[1+\delta_1\alpha_s(\mu^2)\right]^{\omega(k)-\omega(n)}\left[\Psi_{n,k}^{\rm MR}(\mu^2) - \Psi_{n,k}^{\rm MR}(\mu_0^2)\right], \end{aligned} \tag{3.24}$$

$$\Psi_{n,n-k}^{\rm MR}(Q^2) \;=\; \frac{\tilde{m}_{n,n-k}}{[\gamma(n)-\gamma(n-k)-1]\,[\alpha_s(Q^2)]^{\gamma(n)-\gamma(n-k)-1}}\,. \tag{3.25}$$

Comparing Eqs. (3.22) and (3.24), we see that $Z_{n,k}^{\rm RG}(\mu^2,\mu_0^2)$ differs from $Z_{n,k}^{\rm MR}(\mu^2,\mu_0^2)$ in two respects:

- It contains a factor $[1+\delta_1\alpha_s(\mu^2)]^{\omega(k)-\omega(n)}$ in the leading term $\Psi_{n,k}(\mu^2)-\Psi_{n,k}(\mu_0^2)$.
- It comprises additional terms of the type $Z_{n,j}(\mu^2,\mu_0^2)\Psi_{j,k}(\mu_0^2)$, which are related to $Z_{n,j}$ bearing a smaller index $j<k$.

IV. EXACT RENORMALIZATION GROUP SOLUTION

Up to this point we have presented only an approximate form of the Ψ-functions (see, Eq. (3.25)), derived from the MR solution, that satisfy the RG equation. Now that we have outlined the basic steps of the RG restoration, we proceed to our analysis of its consequences for the $\Psi_{n,k}(\mu^2)$-functions. Substituting our solution (3.22) into the two-loop ERBL equation (2.23), we obtain[2]

$$
\begin{aligned}
&(1+\delta_1\alpha_s)\, e_n(\alpha_s) \sum_{0\le j<n}{}' \frac{dZ^{\rm RG}_{n,j}(\alpha_s,\alpha_0)}{d\alpha_s}\, a_j(\alpha_0)\, e_j^{-1}(\alpha_0) \;=\\
&= -\sum_{0\le j<n}{}' \frac{M_{j,n}}{8\pi b_0}\, e_j(\alpha_s) \left[a_j(\alpha_0) e_j^{-1}(\alpha_0) + \sum_{0\le k<j}{}' Z^{\rm RG}_{j,k}(\alpha_s,\alpha_0)\, a_k(\alpha_0) e_k^{-1}(\alpha_0) \right] . \qquad (4.1)
\end{aligned}
$$

Changing indices of summation in the double sum from j,k to k,j and rearranging them as to sum first over j, we obtain due to the arbitrariness of $a_j(\alpha_0)$:

$$
(1+\delta_1\alpha_s)\, e_n(\alpha_s) \frac{dZ^{\rm RG}_{n,j}(\alpha_s,\alpha_0)}{d\alpha_s} = -\tilde{m}_{n,j}\, e_j(\alpha_s) - \sum_{j<k<n}{}' \tilde{m}_{n,k}\, Z^{\rm RG}_{k,j}(\alpha_s,\alpha_0) e_k(\alpha_s)\,. \qquad (4.2)
$$

For $j=n-2$ this differential equation reduces to

$$
-\frac{dZ^{\rm RG}_{n,n-2}(\alpha,\alpha_0)}{d\alpha} \;=\; \tilde{m}_{n,n-2} \frac{e_{n-2}(\alpha)}{e_n(\alpha)\,(1+\delta_1\alpha)}\,, \qquad (4.3)
$$

whose exact solution is

$$
Z^{\rm RG}_{n,n-2}(\alpha,\alpha_0) = \Psi^{\rm RG}_{n,n-2}(\alpha) - \Psi^{\rm RG}_{n,n-2}(\alpha_0) \qquad (4.4)
$$

with

$$
\begin{aligned}
\Psi^{\rm RG}_{n,n-2}(\alpha) \;&=\; \Phi^{\rm RG}_{n,n-2}(\alpha)\;; & (4.5a)\\
\Phi^{\rm RG}_{n,j}(\alpha) \;&\equiv\; \tilde{m}_{n,j} \frac{{}_2F_1\left(1-\gamma(n)+\gamma(j), 1+\omega(n)-\omega(j), 2-\gamma(n)+\gamma(j), -\delta_1\alpha\right)}{[\gamma(n)-\gamma(j)-1]\,\alpha^{\gamma(n)-\gamma(j)-1}}\,. & (4.5b)
\end{aligned}
$$

By definition, the function $\Phi^{\rm RG}_{n,k}(\alpha)$ satisfies the following evolution equation:

$$
\frac{d\Phi^{\rm RG}_{n,j}(\alpha)}{d\alpha} \;=\; -\,\frac{\tilde{m}_{n,j}\; e_j(\alpha)}{e_n(\alpha)\,(1+\delta_1\alpha)}\,. \qquad (4.6)
$$

In Fig. 1 we show both solutions, $Z^{\rm RG}_{2,0}(\alpha,\alpha_0)$ and $Z^{\rm MR}_{2,0}(\alpha,\alpha_0)$, for $\alpha<\alpha_0=0.5$. We observe that the error in $Z_{2,0}(\alpha,\alpha_0)$, when using the approximate MR solution, varies from 25% ($\alpha\approx\alpha_0$) to 15% ($\alpha\to 0.1$).

[2] From now on we trade all the μ^2-dependence for an α_s-dependence (with $\alpha_0=\alpha_s(\mu_0^2)$).

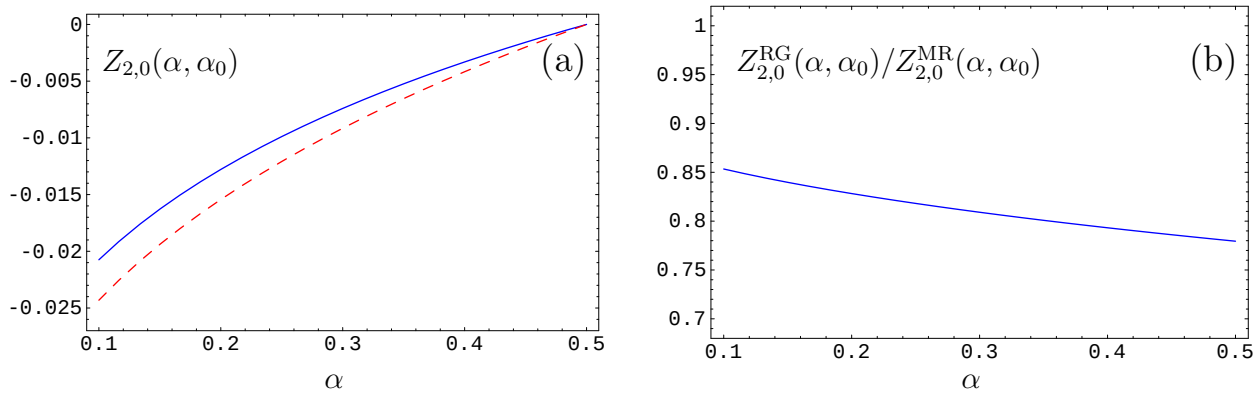

FIG. 1: (a) The solid line corresponds to $Z^{\rm RG}_{2,0}(\alpha,\alpha_0)$ (RG-improved case) and the dashed line to $Z^{\rm MR}_{2,0}(\alpha,\alpha_0)$ (MR-approximate case). (b) The ratio $Z^{\rm RG}_{2,0}(\alpha,\alpha_0)/Z^{\rm MR}_{2,0}(\alpha,\alpha_0)$ is plotted vs. α. In both panels we use $\alpha_0 = 0.5$.

Consider now Eq. (4.2) in the general case $k = n - j$ with $2 \le j < n$. We have the RG representation of its solution (3.22), which can be substituted into the evolution equation (4.2) to obtain[3]

$$\frac{d\Psi_{n,j}(\alpha)}{d\alpha} = -\tilde{m}_{n,j}\frac{e_j(\alpha)}{e_n(\alpha)\,(1+\delta_1\alpha)} - {\sum_{j<k<n}}' \tilde{m}_{n,k}\frac{\Psi_{k,j}(\alpha)e_k(\alpha)}{e_n(\alpha)\,(1+\delta_1\alpha)}\,. \tag{4.7}$$

The solution of this equation can be represented in terms of quadratures:

$$\Psi^{\rm RG}_{n,j}(\alpha) = \Phi^{\rm RG}_{n,j}(\alpha) - {\sum_{j<k<n}}' \tilde{m}_{n,k}\int_0^\alpha \frac{\Psi^{\rm RG}_{k,j}(a)e_k(a)}{e_n(a)\,(1+\delta_1 a)}d\,a\,. \tag{4.8}$$

Before analyzing this solution, let us sketch the procedure to derive it.

- We analyzed the NLO evolution equations (2.23).
- We used for $a_n(\mu^2)$ the representation (3.20) in terms of $Z^{\rm RG}_{n,j}(\mu^2,\mu_0^2)$ and obtained Eq. (4.2).
- We employed the RG representation (3.22) for $Z^{\rm RG}_{n,j}(\mu^2,\mu_0^2)$ and derived this way Eq. (4.7) which yields for $\Psi^{\rm RG}_{n,j}(\alpha)$ an explicit solution given by expression (4.8).

An exact solution of this equation for the case $k = n - 2$ is provided by $\Phi^{\rm RG}_{n,n-2}(\alpha)$, (4.5b), expressed in terms of the hypergeometric function ${}_2F_1\,(a,b,1+a,-\delta_1\alpha)$ with $a = 1-\gamma(n)+\gamma(n-2)$ and $b = 1+\omega(n)-\omega(n-2)$. From Eq. (4.8) we can restore the leading asymptotics of $\Psi^{\rm RG}_{n,j}(\alpha)$ to get

$$\Psi^{\rm RG}_{n,j}(\alpha) \stackrel{\alpha\to 0}{\to} \alpha^{1+\gamma(j)-\gamma(n)}\,, \tag{4.9}$$

a form dictated by the $\Phi^{\rm RG}_{n,j}(\alpha)$-term, whereas the term containing the $\sum'$ in Eq. (4.8) generates a correction with the asymptotics $\alpha^{2+\gamma(j)-\gamma(n)}$. This property allows us to suggest an

[3] We use here the same trick of interchanging summation indices $(j,k) \to (k,j)$ and performing the sums in j and k, as in Appendix B.

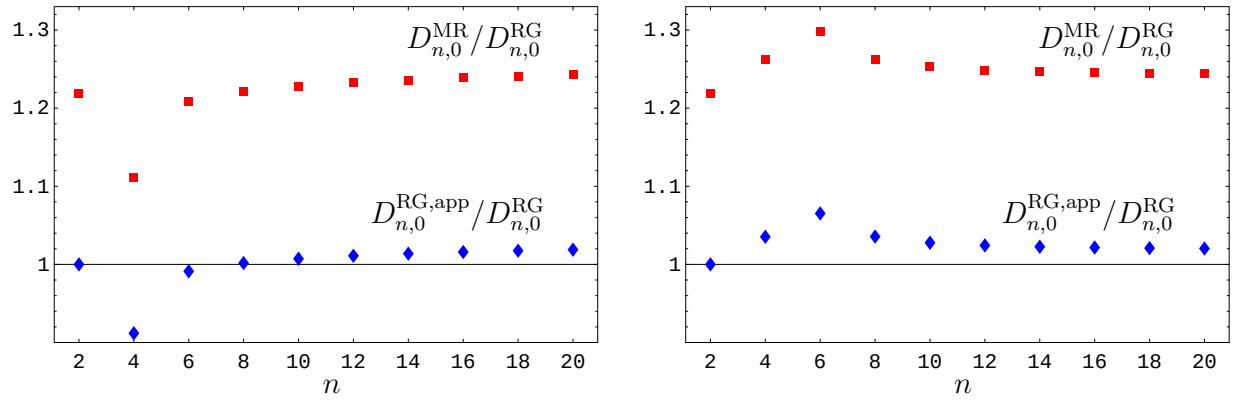

FIG. 2: Comparison of the RG improved, RG approximated, and original MR evolution in terms of the coefficients $D_{n,0}(\alpha_1,\alpha_0)$ with $\alpha_1=\alpha_s(4\ \mathrm{GeV}^2)$ and $\alpha_0=\alpha_s(1\ \mathrm{GeV}^2)$. The blue points at the bottom denote $D^{\rm RG}_{n,0}(\alpha_1,\alpha_0)/D^{\rm MR}_{n,0}(\alpha_1,\alpha_0)$, whereas the red points above them represent $D^{\rm RG}_{n,0}(\alpha_1,\alpha_0)/D^{\rm RG,app}_{n,0}(\alpha_1,\alpha_0)$. Left panel: The original values of $M_{k,n}$ with $M_{0,4}=0.285$ are used. Right panel: All coefficients $M_{k,n}$ have the original values, except for $M_{0,4}$ for which we set $M_{0,4}=-0.8$.

approximate RG solution of the NLO evolution equation (indicated below by the superscript 'app'); viz.,

$$\Psi^{\rm RG,app}_{n,k}(\alpha) \;=\; \Phi^{\rm RG}_{n,k}(\alpha)\,; \tag{4.10}$$

$$Z^{\rm RG,app}_{n,k}(\alpha,\alpha_0) \;=\; \Phi^{\rm RG}_{n,k}(\alpha)-\Phi^{\rm RG}_{n,k}(\alpha_0)\,. \tag{4.11}$$

The results for the coefficients $D_{n,0}(\alpha_1,\alpha_0)$ are shown in Fig. 2. As already mentioned, the RG-approximate evolution is rather good for $n\geq 6$, but for $n=4$ it drops to a much too low value compared to the exact RG-improved result. The reason for this "jump" can be traced to the (unexpected) smallness and positiveness of $M_{0,4}=0.285$, relative to $M_{0,2}=-6.01$ and $M_{2,4}=-17.05$, cf. Eq. (A.6). To show that this jump is connected to the particular value of $M_{0,n}=0.285$ at $n=4$, and is not a numerical error, we show in the right panel of Fig. 2 a graphics, where we set by hand the value of $M_{0,n}=-0.8$. As one sees, the result of this rough simulation yields to a complete cancellation of the dip at $n=4$ turning it into a slight bump at $n=6$, proving the consistency of our numerical algorithm.

The numerical solution of Eq. (4.8) proceeds through the following step-by-step procedure:

- Given that we know the solution for $j=n-2$—supplied by $\Psi^{\rm RG}_{n,n-2}(\alpha)=\Phi^{\rm RG}_{n,n-2}(\alpha)$, cf. Eq. (4.5b)—we determine $\Psi^{\rm RG}_{n-2,n-4}(\alpha)$ and solve numerically Eq. (4.8) for $j=n-4$. This yields

$$\Psi^{\rm RG}_{n,n-4}(\alpha)=\Phi^{\rm RG}_{n,n-4}(\alpha)-\tilde{m}_{n,n-2}\int_{\alpha_\infty}^{\alpha}\frac{\Psi^{\rm RG}_{n-2,n-4}(a)e_{n-2}(a)}{e_n(a)\,(1+\delta_1 a)}d\,a\,.$$

- We then solve numerically Eq. (4.8) for $j=n-k$ using the results $\{\Psi^{\rm RG}_{n-k+2,n-k}(\alpha),\ldots,\Psi^{\rm RG}_{n-2,n-k}(\alpha)\}$ of the previous steps to get $\Psi^{\rm RG}_{n,n-k}(\alpha)$.

- Finally, we solve numerically Eq. (4.8) for $j=0$, employing $\{\Psi^{\rm RG}_{2,0}(\alpha),\ldots,\Psi^{\rm RG}_{n-2,0}(\alpha)\}$ to find $\Psi^{\rm RG}_{n,0}(\alpha)$.

This procedure is repeated for all values of n, starting with $n=2$, continuing with $n=4$, and so on. The upshot of this procedure, $Z^{\rm RG}_{4,0}(\alpha,\alpha_0)$, is shown in Fig. 3 in comparison with

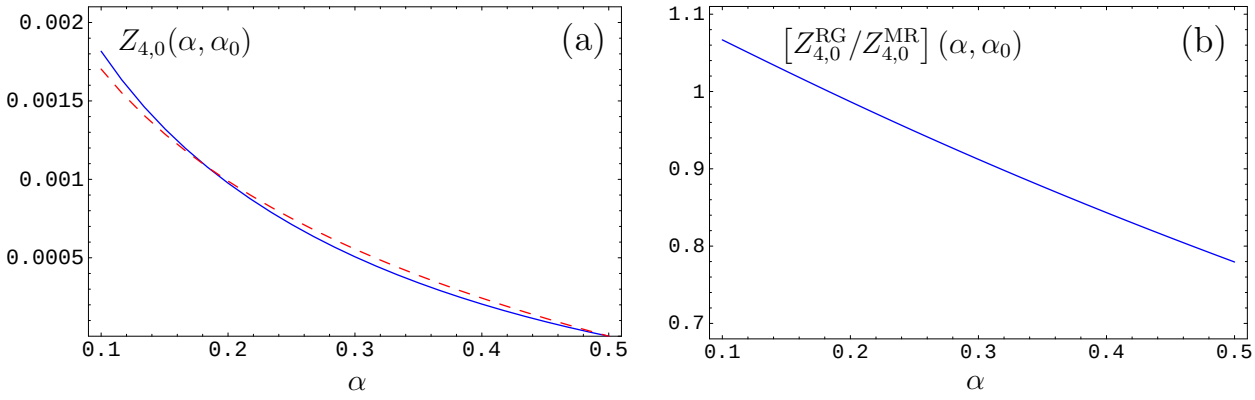

FIG. 3: (a) The solid line corresponds to $Z^{\rm RG}_{4,0}(\alpha,\alpha_0)$ and the dashed line to $Z^{\rm MR}_{4,0}(\alpha,\alpha_0)$. (b) The ratio $Z^{\rm RG}_{4,0}(\alpha,\alpha_0)/Z^{\rm MR}_{4,0}(\alpha,\alpha_0)$ vs. α is shown. We use in both panels $\alpha_0 = 0.5$.

the approximate MR solution $Z^{\rm MR}_{4,0}(\alpha,\alpha_0)$, using in both cases $\alpha < \alpha_0 = 0.5$. One notes that the error in $Z_{4,0}(\alpha,\alpha_0)$ induced by the MR approximation is quite substantial, varying from $+20\%$ ($\alpha \approx \alpha_0$) to -5% ($\alpha \to 0$).

V. NUMERICAL IMPORTANCE OF THE RENORMALIZATION GROUP SOLUTION

Let us now outline the importance of the RG improvement in terms of the evolution of the one-loop asymptotic DA using the MR scheme and the RG-improved one in comparison and continue then to the more complicated case of a double-humped, endpoint-suppressed pion DA obtained in [15]. The asymptotic solution to the one-loop evolution equation reads

$$\varphi_\pi(x,\mu_0^2 = 1\ {\rm GeV}^2) \;=\; \varphi_{\rm as}(x) \;=\; 6x(1-x)\,; \qquad a_n(\mu_0^2) = \begin{cases} 1 & \text{if } n=0 \\ 0 & \text{if } n\neq 0 \end{cases}. \tag{5.1}$$

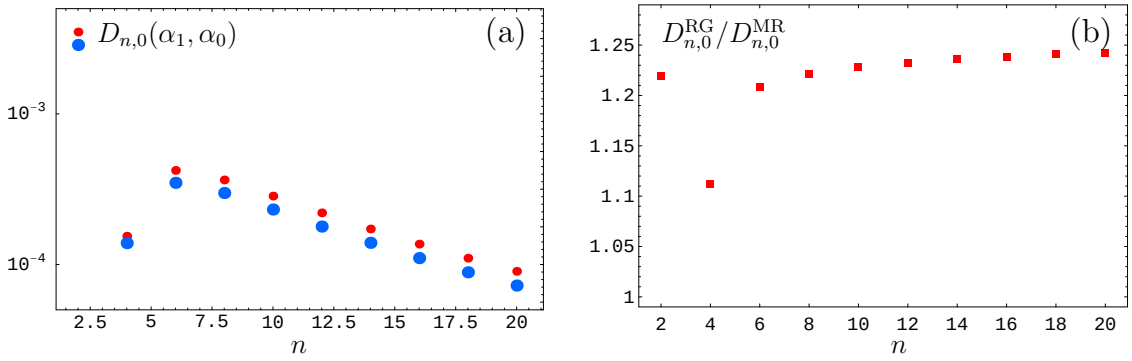

FIG. 4: Comparison of the RG-improved evolution coefficients $D_{n,0}(\alpha_1,\alpha_0)$ with $\alpha_1 = \alpha_s(4\ {\rm GeV}^2)$ and $\alpha_0 = \alpha_s(1\ {\rm GeV}^2)$ contrasted to the MR-approximate version. (a) The blue points denote $D^{\rm RG}_{n,0}(\alpha_1,\alpha_0)$, whereas the red points mark $D^{\rm MR}_{n,0}(\alpha_1,\alpha_0)$ (note the logarithmic scale used for the ordinate.) (b) The ratio $D^{\rm RG}_{n,0}(\alpha_1,\alpha_0)/D^{\rm MR}_{n,0}(\alpha_1,\alpha_0)$ as a function of the order number n is shown.

Then, in accordance with (3.13), we have

$$a_n(Q^2) \;=\; \begin{cases} 1 & \text{if } n=0 \\ e_n(Q^2) Z_{n,0}(Q^2,\mu_0^2) = D_{n,0}(Q^2,\mu_0^2) & \text{if } n\neq 0 \end{cases} . \tag{5.2}$$

Figure 4(a) shows the comparison of the two evolution schemes for the coefficients $D_{n,0}(Q^2,\mu_0^2)$ for $Q^2 = 4$ GeV^2 with $n = 2,\ldots,20$, whereas the ratio of these coefficients is displayed in Fig. 4(b).

Two observations are worth noting:

(i) The absolute difference $D_{n,0}^{\rm MR}(4\ {\rm GeV}^2, 1\ {\rm GeV}^2) - D_{n,0}^{\rm RG}(4\ {\rm GeV}^2, 1\ {\rm GeV}^2)$ for all n is small (being of order α_s—Eq. (3.2)).

(ii) The achieved improvement is high, reaching a level of reduction of the evolution coefficients of up to 20%.

The next step of the analysis involves the comparison of the results of the RG and MR evolution approaches as applied to the pion DA itself—Fig. 5—taking into account the first 100 nontrivial terms, meaning summing up $n = 2, 4, \ldots 200$ higher Gegenbauer harmonics. In panel (a) we display the function $\varphi(x)/x$ in the vicinity of the endpoint $x = 0$, whereas in panel (b) we show the DA around the middle point $x = 0.5$. The key observation here is that in both panels, (a) and (b), the RG-improved approach produces slightly smaller results. More precisely, the DA gradient for the DA value turns out to be smaller by 4% at the origin and by 0.1% at the middle point $x = 0.5$.

In our recent papers with S. V. Mikhailov [16], dealing with the extraction of constraints on the Gegenbauer coefficients of the pion DA from the CLEO data [17] on the $\gamma^*\gamma \to \pi$ transition form factor $F_{\gamma^*\gamma\pi^0}(Q^2)$, we used the standard MR approach to evolve the pion DA [15] from the normalization scale $\mu_0^2 \simeq 1$ GeV^2 to the scale $\mu_{\rm SY}^2 = 5.76$ GeV^2, introduced in [18] by Schmedding and Yakovlev (SY), as being relevant for the CLEO experiment. These results are compiled in Table I. One appreciates that the evolution improvement here due to the RG modification is of minor importance, reaching just the order of 1%.

In Fig. 6(a) we show the same sort of comparison for the truncated inverse moment:

$$\langle x^{-1}\rangle_n \;=\; 3\sum_{j\le n} a_j(Q^2)\,. \tag{5.3}$$

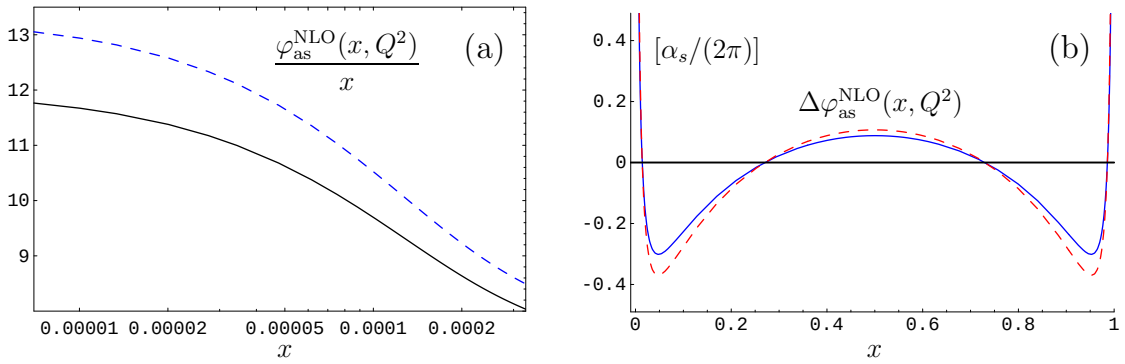

FIG. 5: The left panel shows the extreme endpoint region close to $x = 0$ to effect the changes entailed by evolution. The right panel shows in units of $\alpha_s/(2\pi)$ the relative NLO correction using the RG-corrected evolution, where $\Delta\varphi_{\rm as}^{\rm NLO}(x,Q^2)$ is defined as $\left[\varphi_{\rm as}^{\rm NLO}(x,Q^2) - \varphi_{\rm as}(x)\right]/\varphi_{\rm as}(x)$. In both panels, the solid line corresponds to the RG-improved evolution, whereas the dashed one represents the MR evolution.

TABLE I: Results of the evolution of the Gegenbauer coefficients a_2 and a_4 from the scale $\mu_0^2 = 1$ GeV^2 to the scale $\mu_{\rm SY}^2 = 5.76$ GeV^2 [18] for the asymptotic, BMS [15], and CZ [10] pion DAs.

DA models	$a_2(\mu_0^2)$	$a_2^{\rm MR}(\mu_{\rm SY}^2)$	$a_2^{\rm RG}(\mu_{\rm SY}^2)$	$a_4(\mu_0^2)$	$a_4^{\rm MR}(\mu_{\rm SY}^2)$	$a_4^{\rm RG}(\mu_{\rm SY}^2)$
As	0	-0.004	-0.003	0	0	0
BMS	0.204	0.144	0.145	-0.144	-0.093	-0.092
CZ	0.56	0.403	0.403	0	-0.004	-0.005

We see that in the RG-improved evolution scheme, $\langle x^{-1}\rangle_n$ approaches the limiting value $\langle x^{-1}\rangle_\infty$, represented by the dashed line, more rapidly.

Note in this context that in a previous analysis with K. Passek-Kumerički and W. Schroers of the pion form factor [19] we have analyzed the NLO evolution of the pion DA in the MR evolution scheme, using the property of the two-loop evolution just described. More precisely, if one is interested only in the value of the inverse moment, as this is exactly the case for the factorized part of the pion form factor, then it is actually enough to use for the calculation the LO evolution (2.10), ensuring this way an accuracy at the 1% level. Indeed, to establish this property, we analyzed in [19] numerically the convergence of the truncated moment $\langle x^{-1}\rangle_n$ up to $n = 100$. In the present RG-improved approach, this property can be established even at lower values of n.

Let us step one level higher and consider now the BMS pion DA

$$\varphi_{\rm BMS}(x) \;=\; 6x(1-x)\,\Big[1 + a_2^{\rm BMS}(\mu_0^2)\,C_2^{3/2}(2x-1) + a_4^{\rm BMS}(\mu_0^2)\,C_4^{3/2}(2x-1)\Big] \qquad (5.4)$$

as the initial input of evolution. Then, in accordance with (3.13), we have

$$a_2^{\rm BMS}(Q^2) \;=\; E_2(Q^2,\mu_0^2)\,a_2^{\rm BMS}(\mu_0^2) + D_{2,0}(Q^2,\mu_0^2)\,; \qquad (5.5)$$
$$a_4^{\rm BMS}(Q^2) \;=\; E_4(Q^2,\mu_0^2)\,a_4^{\rm BMS}(\mu_0^2) + D_{4,0}(Q^2,\mu_0^2) + D_{4,2}(Q^2,\mu_0^2)\,a_2^{\rm BMS}(\mu_0^2)\,. \qquad (5.6)$$

All higher coefficients at the initial point $\mu_0^2 = 1$ GeV^2 vanish and therefore we have

$$a_{n\geq 6}^{\rm BMS}(Q^2) \;=\; D_{n,0}(Q^2,\mu_0^2) + D_{n,2}(Q^2,\mu_0^2)\,a_2^{\rm BMS}(\mu_0^2) + D_{n,4}(Q^2,\mu_0^2)\,a_4^{\rm BMS}(\mu_0^2)\,. \qquad (5.7)$$

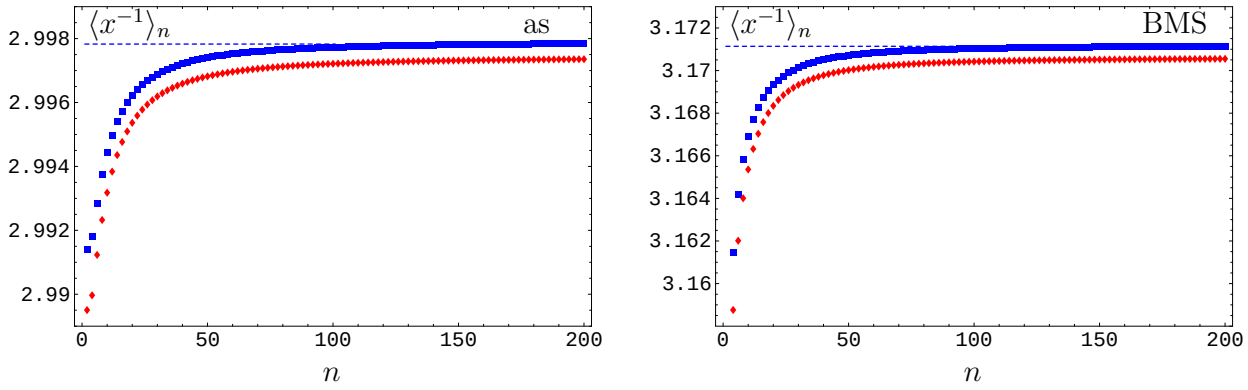

FIG. 6: The impact on the asymptotic pion DA and the BMS one (indicated by corresponding acronyms) of the RG-improved evolution (blue squares on the top) relative to the MR evolution (red diamonds) on the truncated inverse moment $\langle x^{-1}\rangle_n$, Eq. (5.3), as a function of the number n of the Gegenbauer harmonics included. The limiting value $\langle x^{-1}\rangle_\infty^{\rm RG}$ (dashed line) is also displayed.

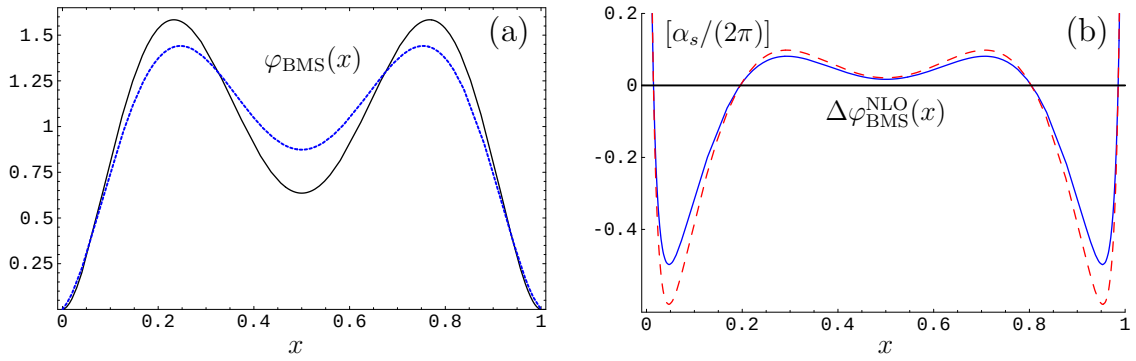

FIG. 7: (a) The effect of the RG-improved evolution (blue dashed line) on the initial BMS pion DA (solid line) is illustrated. (b) We show in units of $\alpha_s/(2\pi)$ the relative NLO correction using on the initial BMS pion DA the RG-improved evolution, the emphasis being placed on the endpoint regions $x = 0$ and $x = 1$. Notice that $\Delta\varphi^{\rm NLO}_{\rm BMS}(x)$ is defined as $\left[\varphi^{\rm NLO}_{\rm BMS}(x,Q^2) - \varphi^{\rm LO}_{\rm BMS}(x)\right]/\varphi_{\rm as}(x)$. For the sake of comparison with Fig. 5, we normalize this expression to $\varphi_{\rm as}(x)$.

Then, in NLO, the BMS pion DA evolved from the scale $\mu_0^2 = 1$ GeV^2 to the scale Q^2, within the RG-improved scheme, is given by

$$\varphi^{\rm NLO}_{\rm BMS}(x,Q^2) \;=\; 6x(1-x)\left[1+\sum_{n\geq 1} a^{\rm BMS}_{2n}(Q^2)\, C^{3/2}_{2n}(2x-1)\right], \tag{5.8}$$

whereas its counterpart in LO, $\varphi^{\rm LO}_{\rm BMS}(x)$, is obtained with the diagonal part given by Eqs. (5.5)–(5.6).

The comparison of the results of the RG-improved and the MR-approximate evolution approaches, as applied to the BMS pion DA, is shown in Fig. 7 taking into account the first 100 nontrivial terms ($n = 2, 4, \ldots, 200$). In panel (a) we display the evolution effect of the RG-improved approach for the BMS pion DA. For the reader's convenience, we use in our analysis the same numerical values $N_f = 3$ and $Q^2 = 4$ GeV^2 as in [9], but employing a higher initial point of evolution $\mu^2 = 1$ GeV^2. The illustration of the evolution effect, especially on the endpoints ($x \to 0$, $x \to 1$), is shown in Fig. 7(b). We will return to this issue and study the influence of the RG-improvement in our discussion of the evolution with a fixed α_s in the next section.

VI. RG SOLUTION IN THE CASE OF A FIXED COUPLING CONSTANT

We turn now to a comparison of our results with those obtained in [9] for the evolution with a fixed α_s, restricting attention to the asymptotic pion DA, the BMS case being analogous. To this end, let us adopt our formulae to this case, using for the corresponding quantities a tilde: $\tilde{e}_n(Q^2)$, $\tilde{Z}_{n,j}(Q^2,\mu^2)$, and $\tilde{\Psi}_{n,j}(Q^2)$. First of all, we realize that we have a different "diagonal" evolution

$$\tilde{E}_n(Q^2,\mu^2) \;=\; \frac{\tilde{e}_n(Q^2)}{\tilde{e}_n(\mu^2)}; \qquad \tilde{e}_n(Q^2) \;=\; \left[\frac{Q_0^2}{Q^2}\right]^{\eta(n)}, \tag{6.1}$$

$$\eta(n) \;\equiv\; \frac{1}{2}\left(\frac{\alpha_s}{4\pi}\right)\left[\gamma_0(n) + \left(\frac{\alpha_s}{4\pi}\right)\gamma_1(n)\right], \tag{6.2}$$

where Q_0^2 is an arbitrary auxiliary scale. Equations (3.19), (3.20), and (3.22) remain valid, but the ERBL equation for $a_n(Q^2)$ gets modified to assume the following form

$$\frac{da_n(Q^2)}{d\ln(Q^2)} = -\eta(n) a_n(Q^2) + \frac{1}{2}\left(\frac{\alpha_s}{4\pi}\right)^2 {\sum_{0\le j<n}}' M_{j,n} a_j(Q^2)\,. \tag{6.3}$$

Equation (4.2) then transforms to

$$\frac{d\tilde{Z}^{\rm RG}_{n,j}(Q^2,\mu^2)}{d\ln Q^2} = \frac{1}{2}\left(\frac{\alpha_s}{4\pi}\right)^2 \left[M_{j,n}\,\frac{\tilde{e}_j(Q^2)}{\tilde{e}_n(Q^2)} + {\sum_{j<k<n}}' M_{k,n}\,\frac{\tilde{e}_k(Q^2)}{\tilde{e}_n(Q^2)}\,\tilde{Z}^{\rm RG}_{k,j}(Q^2,\mu^2)\right] \tag{6.4}$$

and for $j = n-2$ it reduces to

$$\frac{d\tilde{Z}^{\rm RG}_{n,n-2}(Q^2,\mu^2)}{d\ln Q^2} = \frac{1}{2}\left(\frac{\alpha_s}{4\pi}\right)^2 M_{n-2,n}\,\frac{\tilde{e}_{n-2}(Q^2)}{\tilde{e}_n(Q^2)}\,. \tag{6.5}$$

Its exact solution reads

$$\tilde{Z}^{\rm RG}_{n,n-2}(Q^2,\mu^2) = \tilde{\Psi}^{\rm RG}_{n,n-2}(Q^2) - \tilde{\Psi}^{\rm RG}_{n,n-2}(\mu^2) \tag{6.6}$$

with

$$\tilde{\Psi}^{\rm RG}_{n,n-2}(Q^2) \;\equiv\; \frac{1}{2}\left(\frac{\alpha_s}{4\pi}\right)^2 \frac{L_{n,n-2}}{\eta(n)-\eta(n-2)}\,\frac{\tilde{e}_{n-2}(Q^2)}{\tilde{e}_n(Q^2)} \tag{6.7a}$$

$$= \left(\frac{\alpha_s}{4\pi}\right) \frac{L_{n,n-2}\;\left[Q^2/Q_0^2\right]^{\eta(n)-\eta(n-2)}}{\gamma_0(n)-\gamma_0(n-2)+\left[\alpha_s/(4\pi)\right]\left(\gamma_1(n)-\gamma_1(n-2)\right)}\,; \tag{6.7b}$$

$$L_{n,n-2} \;=\; M_{n-2,n}\,. \tag{6.7c}$$

But for this solution we have already obtained a RG-improved expression, given by (3.22). After substituting this expression into the evolution equation (6.4), we obtain

$$\frac{d\tilde{\Psi}_{n,j}(Q^2)}{d\ln Q^2} = \frac{1}{2}\left(\frac{\alpha_s}{4\pi}\right)^2 \left[M_{j,n}\,\frac{\tilde{e}_j(Q^2)}{\tilde{e}_n(Q^2)} + {\sum_{j<k<n}}' M_{k,n}\tilde{\Psi}_{k,j}(Q^2)\frac{\tilde{e}_k(Q^2)}{\tilde{e}_n(Q^2)}\right]\,. \tag{6.8}$$

The solution of this differential equation can be represented as

$$\tilde{\Psi}^{\rm RG}_{n,j}(Q^2) \;\equiv\; \frac{1}{2}\left(\frac{\alpha_s}{4\pi}\right)^2 \frac{L_{n,j}}{\eta(n)-\eta(j)}\,\frac{\tilde{e}_j(Q^2)}{\tilde{e}_n(Q^2)} \tag{6.9a}$$

$$= \left(\frac{\alpha_s}{4\pi}\right) \frac{L_{n,j}\;\left[Q^2/Q_0^2\right]^{\eta(n)-\eta(j)}}{\gamma_0(n)-\gamma_0(j)+\left[\alpha_s/(4\pi)\right]\left(\gamma_1(n)-\gamma_1(j)\right)}\,, \tag{6.9b}$$

where the matrix $L_{n,j}$ is defined iteratively by

$$L_{n,j} = M_{j,n} + \frac{1}{2}\left(\frac{\alpha_s}{4\pi}\right)^2 {\sum_{j<k<n}}' M_{k,n}\frac{L_{k,j}}{\eta(k)-\eta(j)}\,. \tag{6.9c}$$

In Fig. 8 we show numerical results for $L_{n,j}$ and $M_{j,n}$. As one sees, the RG-improved solution $L_{n,j}$ is for $1 \ll j \le n-2$ 3 to 4 times smaller compared to $M_{j,n}$.

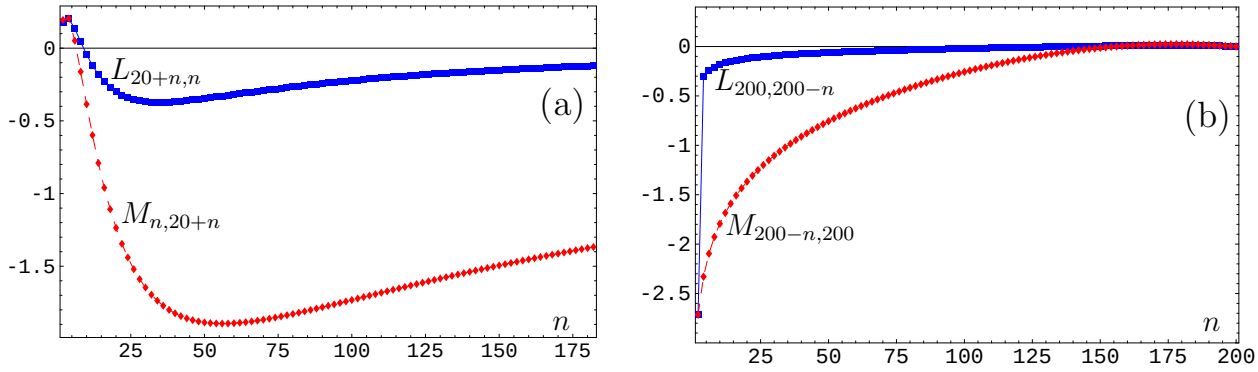

FIG. 8: Comparison of $L_{n,j}$ and $M_{j,n}$ for fixed $\alpha_s = 0.5$. (a) The case of a fixed difference $n - j = 20$ is shown. (b) An analogous situation is shown for $n = 200$.

Having obtained these exact solutions, it is instructive to see how the result derived in [9] for the asymptotic ($Q^2 \to \infty$) solution of the NLO ERBL equation with fixed α_s can be reproduced. From Eq. (3.20) we know that the Q^2-dependence of the Gegenbauer expansion coefficients a_n is determined by the combinations $\tilde{e}_n(Q^2)\tilde{e}_n^{-1}(\mu^2)$ and $\tilde{e}_n(Q^2)\tilde{Z}^{\rm RG}_{n,j}(Q^2,\mu^2)\tilde{e}_j^{-1}(\mu^2)$. The first term has an evident asymptotics:

$$\frac{\tilde{e}_n(Q^2)}{\tilde{e}_n^{-1}(\mu^2)} \;=\; \left[\frac{\mu^2}{Q^2}\right]^{\eta(n)} \;\stackrel{Q^2\to\infty}{\to}\; \begin{cases} 1, & \text{if } n = 0 \\ 0, & \text{if } n \neq 0 \end{cases}, \tag{6.10}$$

whereas the asymptotics of the second term can be determined as follows. First, let us determine the asymptotics of this term in the case $j = j_2 \equiv n - 2$:

$$\tilde{e}_n(Q^2)\tilde{Z}^{\rm RG}_{n,j_2}(Q^2,\mu^2)\tilde{e}_{j_2}(\mu^2)^{-1} = \frac{1}{2}\left(\frac{\alpha_s}{4\pi}\right)^2 \left[\left(\frac{\mu^2}{Q^2}\right)^{\eta(j_2)} - \left(\frac{\mu^2}{Q^2}\right)^{\eta(n)}\right] \frac{L_{n,j_2}}{\eta(n) - \eta(j_2)}\,.$$

For $Q^2 \to \infty$ we have

$$\tilde{e}_n(Q^2)\tilde{Z}^{\rm RG}_{n,j_2}(Q^2,\mu^2)\tilde{e}_{j_2}(\mu^2)^{-1} \;\to\; \begin{cases} \dfrac{1}{2}\left(\dfrac{\alpha_s}{4\pi}\right)^2 \dfrac{L_{n,0}}{\eta(n)}, & \text{if } j_2 = 0 \\ 0, & \text{if } j_2 \neq 0 \end{cases}. \tag{6.11}$$

The case $j = j_4 \equiv n - 4$ differs from the case $j = j_2$ by the contribution of an additional term; viz.,

$$\left[\tilde{e}_n(Q^2)\,\tilde{Z}_{n,j_2}(Q^2,\mu^2)\,\tilde{e}_{j_2}(\mu^2)^{-1}\right]\,\tilde{\Psi}_{j_2,j_4}(\mu^2)\,\frac{\tilde{e}_{j_2}(\mu^2)}{\tilde{e}_{j_4}(\mu^2)}\,, \tag{6.12}$$

which vanishes as $Q^2 \to \infty$ due to Eq. (6.11) and $j_2 > j_4 \geq 0$. The same conclusion can be drawn for all $j = n - k$ with $k \geq 4$, so that we can state that for $Q^2 \to \infty$

$$\tilde{e}_n(Q^2)\tilde{Z}^{\rm RG}_{n,j}(Q^2,\mu^2)\tilde{e}_j(\mu^2)^{-1} \;\to\; \begin{cases} \left(\dfrac{\alpha_s}{4\pi}\right) \dfrac{L_{n,0}}{\gamma_0(n) + (\alpha_s/4\pi)\gamma_1(n)}, & \text{if } j = 0 \\ 0, & \text{if } j \neq 0 \end{cases}. \tag{6.13}$$

Then, in accordance with Eq. (3.20), the new (non-polynomial) asymptotic distribution amplitude is given by

$$\varphi_{\rm as}^{\rm NLO}(x;\alpha_s) \;=\; \varphi_{\rm as}(x)\left[1 + \left(\frac{\alpha_s}{4\pi}\right) {\sum_{n\geq 2}}' \frac{L_{n,0}}{\gamma_0(n) + (\alpha_s/4\pi)\gamma_1(n)}\, C_n^{3/2}(2x-1)\right]. \tag{6.14}$$

Expanding this expression in α_s and retaining only the $O(\alpha_s)$-terms, we obtain

$$\varphi_{\rm as}^{\rm NLO}(x;\alpha_s) \;=\; \varphi_{\rm as}(x)\left[1+\left(\frac{\alpha_s}{4\pi}\right)\sum_{n\geq 2}{}'\,\frac{M_{0,n}}{\gamma_0(n)}\,C_n^{3/2}(2x-1)\right]+O(\alpha_s^2)\,. \tag{6.15}$$

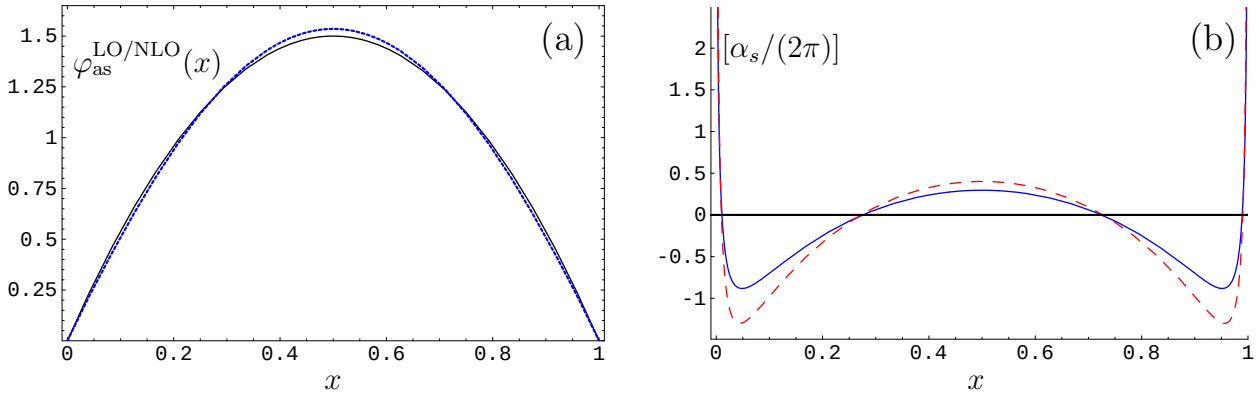

FIG. 9: Evolution of the pion DA for fixed $\alpha_s = 0.5$ and three active flavors. As a nonperturbative input at $\mu_0^2 = 0.25$ GeV^2 we take the asymptotic DA $\varphi_{\rm as}(x)$ in the leading order. (a) The LO asymptotic DA, $\varphi_{\rm as}(x)$, (solid line) in comparison with the exact NLO asymptotic DA $\varphi_{\rm as}^{\rm NLO}(x,\alpha_s)$ (Eq. (6.14), dashed line). (b) The relative NLO corrections to $\varphi_{\rm as}(x,Q^2)$ at $Q^2 = 4$ GeV^2 are shown in units of $\alpha_s/(2\pi)$ following [9] for an easier comparison: the exact RG prediction, Eqs. (6.9a)–(6.9c), is denoted by a solid line and the result of [9], Eq. (6.16a), is represented by a dashed line.

Using the explicit form of $M_{0,n}$—see Eqs. (A.7)–(A.9)—this expression can be recast in the form

$$\varphi_{\rm as}^{\rm NLO}(x;\alpha_s) \;=\; \varphi_{\rm as}(x)\left[1+\frac{\alpha_s}{4\pi}\,\big(C_F\phi_F(x)+b_0\phi_{b_0}(x)\big)\right]+O(\alpha_s^2) \tag{6.16a}$$

which coincides with Eq. (31) derived in Ref. [9]. Here, the following abbreviations have been introduced

$$\begin{aligned}\phi_F(x) \;&\equiv\; \sum_{n\geq 2}{}'\,\frac{4\,(2n+3)}{(n+1)(n+2)}\left[\frac{4A_{n0}}{n(n+3)}+A_{n0}-\psi(n+2)+\psi(1)\right]C_n^{3/2}(2x-1)\\ &=\; \ln^2\left[\frac{1}{x}-1\right]+2-\frac{\pi^2}{3}\,;\end{aligned} \tag{6.16b}$$

$$\phi_{b_0}(x) \;\equiv\; \sum_{n\geq 2}{}'\,\frac{-4\,(2n+3)}{n(n+1)(n+2)(n+3)}\,C_n^{3/2}(2x-1) \;=\; \ln\left[x(1-x)\right]+\frac{5}{3}\,. \tag{6.16c}$$

Hence, we conclude that in the fixed α_s case our approach fully reproduces the two-loop result of Ref. [9] and the part (6.16c) coincides with Mikhailov's finding in [20]. But our approach contains more information. Because of the RG improvement, Eq. (6.14) contains the coefficients $L_{n,0}$ instead of $M_{0,n}$ entering this equation in the approach of [9]—cf. Eq. (6.15). The advantage of the coefficients $L_{n,0}$ is that they are much smaller, as we clearly see from Fig. 8 by comparing the two approaches. In Fig. 9 we show the comparison of the two approaches for the pion DA itself. Note that in our analysis we use the same numerical values $\alpha_s = 0.5$, $N_f = 3$, $\mu^2 = 0.25$ GeV^2, and $Q^2 = 4$ GeV^2 as in [9] and take into

account in Eq. (3.20) the first 100 nontrivial terms ($n = 2, 4, \ldots, 200$) to approximate the evolved distribution amplitude. It is important to stress that our results, obtained in the $\overline{\rm MS}$ scheme of perturbative QCD for a fixed coupling, can be related to those derived before by Müller [21, 23] in the conformally covariant subtraction (CS) scheme. More specifically, the solutions of the ERBL evolution equation in each scheme can be interlinked in the conformal limit ($\beta = 0$) on account of a finite refactorization [21]. This means that our solution (6.16a) in the $\overline{\rm MS}$ scheme and Müller's corresponding results in the CS scheme [21, 23] are connected by a RG transformation matrix determined by the special conformal anomaly [24].

VII. CONCLUSIONS

In this paper we analyzed the ERBL evolution equation for the meson distribution amplitude at the two-loop level. Our main conclusions can be summarized as follows.

- We worked out a procedure to solve the ERBL evolution equation in the NLO approximation, Eqs. (3.20), (3.22), which ensures the RG properties.
- Using this method, we obtained a RG-improved solution of the NLO ERBL evolution equation in the form of quadratures, Eqs. (4.8), (4.5b).
- We worked out an approximate version of our procedure, given by Eqs. (4.10) and (4.11), which is completely analytical. Its accuracy is rather high with an uncertainty of the order of only a few %, except for the case of $Z_{4,0}$, for which the error is about -10%.
- We analyzed the importance of the NLO evolution for the inverse moment of the meson distribution amplitude. We confirmed the conclusion drawn in [19] that it is possible to use the LO evolution for this quantity with the induced overall error being smaller than 1%.

The most discernible theoretical result of this investigation is that the RG-improved evolution is slower and the higher harmonics stronger suppressed relative to the approximate MR scheme, enhancing the self-consistency of QCD perturbation theory.

Acknowledgments

This work was supported in part by the Russian Foundation for Fundamental Research (grants 03-02-16816, 03-02-04022 and 05-01-00992), the Heisenberg–Landau Programme, and the Deutsche Forschungsgemeinschaft (DFG) (grant 436 RUS 113/752/0-1). We are particularly grateful to S. V. Mikhailov for stimulating discussions that inspired us to investigate this subject. We would also like to thank to K. Passek-Kumerički for useful discussions and remarks. One of us (A.P.B.) is grateful to Prof. Klaus Goeke for the warm hospitality at Bochum University, where part of this work was carried out.

APPENDIX A: BETA-FUNCTION AND ANOMALOUS DIMENSIONS

The standard β-function coefficients are given by

$$b_0 = \frac{11N_c - 2N_f}{3}\,; \quad b_1 = \frac{34}{3}N_c^2 - \left(2C_{\rm F} + \frac{10}{3}N_c\right)N_f\,. \tag{A.1}$$

To one-loop, the anomalous dimensions read

$$\gamma_0(n) = 2C_F\left[4\sum_{i=1}^{n+1}\frac{1}{i} - 3 - \frac{2}{(n+1)(n+2)}\right], \tag{A.2}$$

whereas the anomalous dimensions for arbitrary n at the two-loop order may be found in [22, 25], with

$$\gamma_1(0) \;=\; 0\,, \qquad \gamma_1(2) \;=\; \frac{34450}{243} - \frac{830}{81}N_f\,, \qquad \gamma_1(4) \;=\; \frac{662846}{3375} - \frac{31132}{2025}N_f\,. \tag{A.3}$$

The normalization of the Gegenbauer polynomials $\psi_n(x)$ with respect to the weight function $\Omega(x) = 6\,x\,(1-x)$ is

$$N_n \;=\; \int_0^1 \Omega(x)\psi_n^2(x)dx \;=\; \frac{3(n+1)(n+2)}{2(2n+3)}\,. \tag{A.4}$$

The values of the first few matrix elements $M_{j,n}$ have been calculated numerically in [3] to be

$$M_{02} = -11.2 + 1.73N_f, \quad M_{04} = -1.41 + 0.565N_f, \quad M_{24} = -22.0 + 1.65N_f\,. \tag{A.5}$$

In particular, for $N_f = 3$, they read

$$M_{02} = -6.01, \quad M_{04} = 0.285, \quad M_{24} = -17.05\,. \tag{A.6}$$

It is worth pointing out here that Müller in Ref. [8] has obtained analytic expressions for the matrix elements $M_{k,n}$ for all values $j = 0, 2, \ldots < n = 2, 4, \ldots$ [4]

$$M_{j,n} \;=\; 2\,\frac{N_j}{N_n}\,C_{n,j}^{(1)}\left[\gamma_0(n) - \gamma_0(j)\right], \tag{A.7}$$

$$C_{n,j}^{(1)} \;=\; (2j+3)\left[\frac{-\gamma_0(j) - 2b_0 + 8C_F A_{n,j}}{2(n-j)(n+j+3)} + \frac{2C_F(A_{n,j} - \psi(n+2) + \psi(1))}{(j+1)(j+2)}\right], \tag{A.8}$$

$$A_{n,j} \;=\; \psi\left(\frac{n+j+4}{2}\right) - \psi\left(\frac{n-j}{2}\right) + 2\psi(n-j) - \psi(n+2) - \psi(1)\,. \tag{A.9}$$

APPENDIX B: PROOF OF Eq. (3.19)

Using the principle of mathematical induction we want to prove that

$$Z_{n,n-k}(Q^2,\mu^2) = \Psi_{n,n-k}(Q^2) - \Psi_{n,n-k}(\mu^2) - {\sum_{0<j<k}}' Z_{n,n-j}(Q^2,\mu^2)\Psi_{n-j,n-k}(\mu^2) \tag{B.1}$$

[4] The function $\psi(z)$ is defined as usual by $\psi(z) = \frac{d}{dz}\ln\Gamma(z)$.

is the solution of Eq. (3.18).

1 We proved this for $k = 2$.

2 Let us assume that it is valid for all $k \leq m-2$ and then prove that it is valid for $k = m$. We have

$$\begin{aligned}
Z(m,Q^2,q^2,\mu^2) &\equiv -Z_{n,n-m}(Q^2,\mu^2) + Z_{n,n-m}(Q^2,q^2) + Z_{n,n-m}(q^2,\mu^2) \;= \\
&= \sum_{0<j<m}{}' Z_{n,n-j}(Q^2,\mu^2)\Psi_{n-j,n-m}(\mu^2) \\
&- \sum_{0<j<m}{}' \left[Z_{n,n-j}(Q^2,q^2)\Psi_{n-j,n-m}(q^2) + Z_{n,n-j}(q^2,\mu^2)\Psi_{n-j,n-m}(\mu^2)\right] \;= \\
&= \sum_{0<j<m}{}' \left[Z_{n,n-j}(Q^2,\mu^2) - Z_{n,n-j}(Q^2,q^2) - Z_{n,n-j}(q^2,\mu^2)\right]\Psi_{n-j,n-m}(\mu^2) \\
&+ \sum_{0<j<m}{}' Z_{n,n-j}(Q^2,q^2)\left[\Psi_{n-j,n-m}(q^2) - \Psi_{n-j,n-m}(\mu^2)\right] .
\end{aligned}$$

Now we can use Eq. (3.19) to rewrite the last line in the previous equation in the following way (on account of $j \leq m-2$ in all sums)

$$\Psi_{n-j,n-m}(q^2) - \Psi_{n-j,n-m}(\mu^2) = Z_{n-j,n-m}(q^2,\mu^2) + \sum_{j<k<m}{}' Z_{n-j,n-k}(q^2,\mu^2)\Psi_{n-k,n-m}(\mu^2) .$$

Then we find

$$\begin{aligned}
Z(m,Q^2,q^2,\mu^2) &= \sum_{0<j<m}{}' \left[Z_{n,n-j}(Q^2,\mu^2) - Z_{n,n-j}(Q^2,q^2) - Z_{n,n-j}(q^2,\mu^2)\right]\Psi_{n-j,n-m}(\mu^2) \\
&+ \sum_{0<j<m}{}' Z_{n,n-j}(Q^2,q^2)Z_{n-j,n-m}(q^2,\mu^2) \\
&+ \sum_{0<k<m}{}' \sum_{k<j<m}{}' Z_{n,n-k}(Q^2,q^2)Z_{n-k,n-j}(q^2,\mu^2)\Psi_{n-j,n-m}(\mu^2) ,
\end{aligned}$$

where in the last line we have introduced new indices $(j,k \to k,j)$. Changing the order of summations in the double sum gives

$$\begin{aligned}
Z(m,Q^2,q^2,\mu^2) &= \sum_{0<j<m}{}' \left[Z_{n,n-j}(Q^2,\mu^2) - Z_{n,n-j}(Q^2,q^2) - Z_{n,n-j}(q^2,\mu^2)\right]\Psi_{n-j,n-m}(\mu^2) \\
&+ \sum_{0<j<m}{}' Z_{n,n-j}(Q^2,q^2)Z_{n-j,n-m}(q^2,\mu^2) \\
&+ \sum_{0<j<m}{}' \sum_{0<k<j}{}' Z_{n,n-k}(Q^2,q^2)Z_{n-k,n-j}(q^2,\mu^2)\Psi_{n-j,n-m}(\mu^2) \;= \\
&= \sum_{0<j<m}{}' \Big[Z_{n,n-j}(Q^2,\mu^2) - Z_{n,n-j}(Q^2,q^2) - Z_{n,n-j}(q^2,\mu^2) \\
&\qquad + \sum_{0<k<j}{}' Z_{n,n-k}(Q^2,q^2)Z_{n-k,n-j}(q^2,\mu^2)\Big]\Psi_{n-j,n-m}(\mu^2) \\
&+ \sum_{0<j<m}{}' Z_{n,n-j}(Q^2,q^2)Z_{n-j,n-m}(q^2,\mu^2) .
\end{aligned}$$

By virtue of $j \leq m-2$ in all sums, we may use Eq. (3.18) for the expression inside the square brackets to show that it is identically equal to zero. Therefore, we find

$$\begin{aligned} Z(m, Q^2, q^2, \mu^2) &\equiv Z_{n,n-m}(Q^2, \mu^2) - Z_{n,n-m}(Q^2, q^2) - Z_{n,n-m}(q^2, \mu^2) \\ &= {\sum_{0<j<m}}' Z_{n,n-j}(Q^2, q^2) Z_{n-j,n-m}(q^2, \mu^2) \,. \end{aligned}$$

This way we obtain just the desired expression, cf. Eq. (3.18). **Q.E.D.**

---

[1] A.V. Efremov and A.V. Radyushkin, Phys. Lett. 94B (1980) 245; Teor. Mat. Fiz. 42 (1980) 147 [Theor. Math. Phys. 42 (1980) 97].

[2] G.P. Lepage and S.J. Brodsky, Phys. Lett. 87B (1979) 359; Phys. Rev. D22 (1980) 2157.

[3] S.V. Mikhailov and A.V. Radyushkin, Nucl. Phys. B273 (1986) 297.

[4] F.M. Dittes and A.V. Radyushkin, Phys. Lett. 134B (1984) 359;
S.V. Mikhailov and A.V. Radyushkin, JINR-P2-83-721 (unpublished).

[5] M.H. Sarmadi, Phys. Lett. 143B (1984) 471.

[6] G.R. Katz, Phys. Rev. D 31 (1985) 652.

[7] S.V. Mikhailov and A.V. Radyushkin, Nucl. Phys. B254 (1985) 89.

[8] D. Müller, Phys. Rev. D49 (1994) 2525.

[9] D. Müller, Phys. Rev. D51 (1995) 3855.

[10] V.L. Chernyak and A.R. Zhitnitsky, Phys. Rept. 112 (1984) 173.

[11] B.A. Magradze, in: Proceedings of the 10th International Seminar Quarks'98, Suzdal, Russia, 18–24 May 1998, eds. F.L. Bezrukov et al. (INR RAS, Moscow, 1999), pp. 158–171.

[12] E. Gardi, G. Grunberg and M. Karliner, JHEP 07 (1998) 007.

[13] N.G. Stefanis, Eur. Phys. J. direct C7 (1999) 1 [hep-ph/9911375].

[14] E.P. Kadantseva, S.V. Mikhailov and A.V. Radyushkin, Yad. Fiz. 44 (1986) 507 [Sov. J. Nucl. Phys. 44 (1986) 326].

[15] A.P. Bakulev, S.V. Mikhailov and N.G. Stefanis, Phys. Lett. B508 (2001) 279 [Erratum-ibid. B590 (2004) 309]; in: Proceedings of the 36th Rencontres De Moriond On QCD And Hadronic Interactions, 17-24 Mar 2001, Les Arcs, France [hep-ph/0104290].

[16] A.P. Bakulev, S.V. Mikhailov and N. G. Stefanis, Phys. Rev. D67 (2003) 074012; Phys. Lett. B578 (2004) 91; in: Proceedings of the 2nd Conference on Nuclear and Particle Physics with CEBAF at Jlab (NAPP 2003), Dubrovnik, Croatia, 26-31 May 2003 [hep-ph/0311140]; Phys. Part. Nucl. 35 (2004) 7 [hep-ph/0312141]; in: Proceedings of the LC03 Workshop On Hadrons and Beyond, 15-9 Aug 2003, Durham, England, ed. S. Dalley (IPPP, Durham, 2003), pp. 172–177 [hep-ph/0310267]; Annalen Phys. 13 (2004) 629.

[17] J. Gronberg et al., Phys. Rev. D57 (1998) 33.

[18] A. Schmedding and O. Yakovlev, Phys. Rev. D62 (2000) 116002;
A. Khodjamirian, Eur. Phys. J. C6 (1999) 477.

[19] A.P. Bakulev, K. Passek-Kumerički, W. Schroers and N.G. Stefanis, Phys. Rev. D70 (2004) 033014; N.G. Stefanis et al., in: Workshop on Hadron Structure and QCD: From Low to High Energies (HSQCD 2004), St. Petersburg, Repino, Russia, 18-22 May 2004, to be published in the proceedings [hep-ph/0409176]; N.G. Stefanis, in: 11th International Conference in Quantum ChromoDynamics (QCD 04), Montpellier, France, 5-9 Jul 2004, to be published in Nucl. Phys. B Suppl. [hep-ph/0410245]; A.P. Bakulev, in: International Bogolyubov Conference on

Problems of Theoretical and Mathematical Physics, Moscow, Russia, 2-6 Sep 2004, to be published in the proceedings [hep-ph/0412248].
[20] S. V. Mikhailov, Phys. Rev. D62 (2000) 034002.
[21] D. Müller, Phys. Rev. D **58** (1998) 054005
[22] E.G. Floratos, D.A. Ross and C.T. Sachrajda, Nucl. Phys. B129 (1977) 66.
[23] D. Muller, Phys. Rev. D **59** (1999) 116003
[24] S. J. Brodsky, P. Damgaard, Y. Frishman and G. P. Lepage, Phys. Rev. D **33** (1986) 1881.
[25] A. Gonzalez-Arroyo, C. Lopez and F.J. Yndurain, Nucl. Phys. B153 (1979) 161.